# Acoustic, mechanical and microstructural properties of extruded crisp bread

Ewa Gondek[a], Ewa Jakubczyk[a], Els Herremans[b], Bert Verlinden[f], Maarten Hertog[b], Thomas Vandendriessche[b], Pieter Verboven[b], Aleksandra Antoniuk[c], Evi Bongaers[d] , Pascal Estrade[e], Bart M. Nicolaï[b]

[a]Department of Food Engineering and Process Management, Warsaw University of Life Sciences, Nowoursynowska 159c, 02-776 Warsaw, Poland

[b]BIOSYST-MeBioS, KU Leuven, Willem de Croylaan 42, B-3001 Leuven, Belgium

[c] Chaber S.A., Al. Prymasa Tysiąclecia 83, 01-242 Warsaw, Poland

[d]Bruker microCT, Kartuizersweg 3B, 2550 Kontich, Belgium

[e]VSG, Avenue Kennedy 87, Mérignac Cedex 33708, France

[f]Flanders Centre of Postharvest Technology, Willem de Croylaan 42, B-3001 Leuven, Belgium

*Corresponding author*: Ewa Jakubczyk, Department of Food Engineering and Process Management, Warsaw University of Life Sciences, Nowoursynowska 159c, 02-776 Warsaw, Poland, tel. +48225937563, e-mail: ewa_jakubczyk@sggw.pl

Key words: extruded bread, texture, acoustic properties, microstructure

**Abstract**

The aim of this work was to describe the texture and structure of crisp bread obtained with different extrusion parameters. The texture of different crisp bread samples was evaluated using a combination of acoustic and mechanical tests. The advantage of this measurement setup is the feasibility of simultaneous registering the force–deformation characteristics, sounds (using an acoustic envelope detector coupled to the texture analyser with a microphone) as well as mechanical vibrations (registered using a piezoelectric sensor) generated during a penetration test. All analysed samples of bread were products with a crisp texture that emitted audible sounds with a significant intensity that could be registered with a microphone as well as with a contact method. The microstructure of extruded bread obtained at the lowest screw speed and the highest feeding rate was characterised by a high number of small regular pores that caused the sensation of product crispness.

## 1. **Introduction**

Texture is one of the most important quality attributes of a food product experienced by consumers. It is often described by both sensory features describing preference (crispness, crunchiness, juiciness, tenderness) that are always associated with freshness, good quality, as well as features that describe dislike (hardness, cloudiness, sliminess) that are associated with bad quality. The texture experience is a complex sensory property perceived through a combination of visual, kinaesthetic, tactile and auditory sensations (Szczesniak, 2002). Although the best texture assessment is carried out by human senses during eating, sensory methods are not convenient for routine analysis. Moreover, the results obtained by different sensory panels are difficult to compare (Roudaut et al., 2002). In recent years, texture research has focused on the development of objective, instrumental methods to measure texture and to express it by objective numerical descriptors (Sealeaw and Schleining, 2011).

Crispness is one of the most important and desirable textural attributes of low moisture food (Duizer, 2001; Varella et al., 2006; Castro-Prada et al., 2009). In the past , many scientists investigated crispness using mechanical tests (penetration, compression, bending), but the force-deformation results often do not show a good correlation with sensory crispness. Furthermore, some food cannot be tested because of their irregular shapes and sizes (Sealeaw and Schleining, 2011). It has been shown that sounds produced during disintegration of the food plays an important role in the perception of texture of food materials (Duizer, 2001; Luyten et al., 2004). Sometimes these sounds describe the overall quality of a food product better than any other sensory feature (Gondek and Marzec, 2008). Mechanical and acoustic evaluation of crispness has been used to describe the texture of biscuits (Chen et. al., 2005), extruded bread (Marzec et al., 2007), roasted almonds (Varela et al., 2006) and apples (Zdunek et al., 2011). The combination of acoustic and force-deformation measurements reveal more information about crispness than any technique alone (Sealeaw and Schleining, 2011). To fully understand how mechanical failure and accompanying acoustic effects occur, knowledge of product microstructure is necessary (Agbisit et al., 2007; Castro-Prada et al., 2009; Sealeaw and Schleining, 2011).

Texture-microstructure relations of foods have already been investigated for dry cellular products such as cornflakes (Gondek et al., 2006), bread crumbs (Zghal et al., 2002), corn starch extrudates (Agbisit et al., 2007), toasted rusk roll (Primo-Martín et al., 2008) and sugar foams (Herremans et al., 2012), as well as for other products (Alamar et al., 2008). The texture of bread is largely determined by its characteristic microstructure (Primo-Martín et al., 2010). Bread has a foam-like structure with walls and pores. The microstructural properties of the bread influence the perceptions of texture, from how the bread looks to how it deforms during handling and mastication (Wang et al., 2011). Until recently, the measurement of food microstructure was essentially based on light or electron microscopy. X-ray micro-computed tomography (micro-CT) is a relatively new technique, which enables the non-destructive visualisation of the internal microstructure of objects. Micro-CT as a non-invasive technique has been applied to the study of the internal 3-D structures of several food products, e.g. marshmallow, aerated chocolate and chocolate muffin (Lim and Barigou, 2004). Babin et al. (2007) studied the microstructure of extruded starches in relation to expansion phenomena and mechanical properties. Verboven et al. (2008) and Herremans et al. (2013) used bench-top and synchrotron micro-CT to evaluate the microstructure of apple fruit in relation to gas exchange properties and internal quality defects. Bakery products such as bread crumbs (Falcone et al., 2004; Wang et al., 2011), and sugar-snap cookies (Pareyt et al., 2009) have been recently investigated using X-ray micro-CT, revealing the arrangement of pores and relating this cellular structure to physical and nutritional properties of the products.

The aim of this work was to describe and analyse the texture and structure of crisp bread obtained with different extrusion parameters. The mechanical properties were measured, and the sound generated during penetration (with application of an acoustic envelope detector - AED) as well as the material vibrations using the contact acoustic emission technique (AE) were recorded and analysed. The results were correlated with morphometric crisp bread parameters obtained with micro-CT.

## 2. Experimental

### 2.1. Materials

The investigated material was extruded crisp bread produced at an industrial scale at pressure 100-120 bar (Chaber, Warsaw, Poland). Four variants of extruded crisp breads were produced from whole grain rye flour and water using different combinations of extrusion parameters, and are further denoted as v.1 (barrel temperature 173°C, screw speed 76 rpm, feeding rate 48 rpm), v.2 (172°C, 76 rpm, 50 rpm), v.3 (114/161°C, 53 rpm, 100 rpm), and v.4 (90/220/166°C, 159 rpm, 26 rpm).

### 2.2. Functional properties

Different functional properties of the crisp bread were measured. The expansion ratio of the extruded breads was computed as a quotient of bread cross-section and extruder jet area. The apparent density of crisp bread samples was estimated by dividing their mass determined by an analytical balance by their volume calculated from their dimensions measured with a caliper. A helium stereopycnometer (Quantachrome Instruments, Boynton Beach, USA) was used to determine the particle (solid) density of crisp bread. Three replicates for each sample were performed for both apparent and particle density measurements.

The water content of the investigated extruded bread was measured according to the Polish Standard PN ISO 6540 by drying at 130°C for 1 hour. The water activity was measured with a HigroLab (Rotronic AG, Bassersdorf, Switzerland) with an accuracy of +/- 0.001 at a temperature of 23±1°C. The Water Solubility Index (WSI) and Water Adsorption Index (WAI) were determined according to the following procedures. The bread samples were ground (M-11basic IKA- Werke GmbH & Co. KG, Staufen, Germany) and a 0.7 g extrudate specimen was suspended in 7ml of distilled water at room temperature (stirring for 30 min), and centrifuged at 250 $s^{-1}$ for 10 min. The supernatant was used to determine WSI (the weight of dry solids in the supernatant expressed as a percentage of the initial weight of the sample). The WAI was calculated as the weight of gel obtained after removal of the supernatant per unit weight of dry solids. Four replicates were measured.

### 2.3. Force-deformation measurements

The mechanical properties of the extruded breads were examined  using of TA-HDplus texture analyser (Stable Micro Systems, Surrey, UK).

Samples of bread (thickness/width/length 7/50/120 mm) were collected directly from the package and subjected to a penetration test using a cylindrical probe (P/36R). The deformation tests were carried out at a constant speed of 1 mm·s$^{-1}$ and up to a strain of 80%. From the force-deformation curve the following parameters were extracted: maximum force (N), area under the force-deformation curve (N·mm), number of force peaks (drop in force higher than 0.8 N), average drop off (the average drop in force between consecutive peaks and troughs, N) and linear distance (the length of a line joining all points in the force-deformation curve).

### 2.4. Acoustic properties

The sound generated by the deformed material was recorded in a non-contact way with an Acoustic Envelope Detector – AED (Stable Micro Systems Godalming, UK) with a free-field microphone 8 mm in diameter (Brüel& Kjær, Naerum, Denmark). The microphone was calibrated using the acoustic calibrator type 4231 (94 and 114 dB SPL, 1000Hz). The detector, mounted to the TA-HDplus texturometer, was working under the Texture Exponent 32 software (Stable Micro Systems Godalming, UK), which enabled simultaneous registration of both the sound signal and changes of force during penetration. Each time, the microphone was fixed at the same distance from the sample (5 cm). Results were recorded at AED detector amplification of AED=3 (12dB) and a frequency of sound sampling reaching 500 Hz. The measuring system enabled measurements of sounds with a frequency in the range of 1-12.5 kHz (Chen et al., 2005). The following characteristics were determined from the sound signal: the number of AED sound peaks (drop in sound pressure level larger than 10dB), the mean of AED sound peaks (the sum of the peaks values divided by number of the peaks, dB), the maximum of AED sound peaks (maximum value of sound pressure level, dB) and the area under the deformation-acoustic signal AED curve( dB·mm).

Between the head of the TA HD plus Texture Analyser and the penetrating tip, a piezoelectric accelerometer was installed in a specially-designed adapter to measure vibrations emitted by the crushed material. Based on preliminary studies, an miniature piezoelectric sensor 4507B (Bruel & Kjaer) was used. An integral amplifier and acoustic background filters were used to measure the sound emitted by the analysed product in a wide frequency range (0.1 – 18kHz) with only minimal interference of the vibrations generated by the texture analyzer. The AE signal was recorded at a sampling frequency of 44.1 kHz using a special analogue-digital processing card type 9112 by Adlink Technology Inc. Descriptors of acoustic emission were determined at a discrimination level of 1000 mV. Analyses were carried out in 25 replications.

### 2.5. Microstructural analysis

The microstructure was imaged by micro-CT. Scans were started immediately after opening the air-tight packages of crisp breads. Prismatic samples with a square cross section were excised from the center of the crisp breads, using a scalpel. The sample height measured 20.0 mm, and width 6.5 mm. The original thickness of the manufactured breads was maintained in preparing the samples. The bread samples were fixed on the rotation stage using kneading dough. Only the part emerging from the fixing substance was used for later image analysis. X-ray micro-CT measurements were performed on a SkyScan 1172 system (Bruker microCT, Kontich, Belgium), operated at 49 keV source voltage and 200 µA current and with an image pixel resolution of 5.9 µm. The samples were rotated over 0.4° steps over a total of 180°, each time averaging 5 frames to acquire a radiographic image of 1048 by 2000 pixels. The final scan duration for each sample was 21 minutes. For each of the four crisp bread variant, 3 individual samples were scanned.

The projection images were loaded into dedicated software (NRecon1.6.3.2, Bruker microCT, Kontich, Belgium) to reconstruct virtual cross-sections of the sample. This resulted in a 3-D greyscale datastack, typically digitized to 900 slices of 2000 by 2000 pixels. The images were smoothed by a Gaussian smoothing kernel, and corrected for rings and beam hardening, which are common artefacts in X-ray CT images.

For image analysis the edges of the datastack were cropped to exclude interference with the excision of the sample. The remaining volume for analysis measured 5 x 5 x 5.32 $mm^3$. The greyscale images were binarised by setting the threshold value at 50 to separate two peaks in the greyscale histogram: pixels with lower intensities were assigned to the background (air) and pixels with a higher intensity were assigned to the crisp bread material. 3D objects smaller than 27 voxels (5.55 x $10^{-6}$ $mm^3$) were considered to be noise and were filtered out of the image. Morphometric parameters describing the microstructure were calculated on the 3-D data using CTAn v.1.10.1.0 (Bruker microCT, Kontich, Belgium). A list of the parameters and the main concept of the calculation are presented in Table 1.

### 2.6. Statistical analysis

The analysis of the morphological data was done in SAS Enterprise Guide (SAS Institute, Cary, NC, USA). One-way analysis of variance (ANOVA) and Tukey's test were used to establish the significance of differences among samples at 95% significance level.

To describe multivariate relations between all measurements, Principal Component Analysis (PCA) was carried out using The Unscrambler software version 10.1 (CAMO Software, Oslo, Norway). As the functional, mechanical and acoustic measurements were done on different samples as those used for the microstructural analysis, an artificial dataset was created in which the first set of measurements were concatenated to a randomly selected set of microstructural features. This was done for three replicates per bread variants. Data were mean-centered and standardized by dividing by its standard deviation.

## 3. Results and discussion

### 3.1. Functional properties

First we wanted to investigate whether the four variants of the crisp bread differed in terms of functional properties. The results are shown in Table 2. Regardless of the extrusion process parameters, always low-density products with low water activity were obtained. The lowest WSI and the highest WAI were observed for bread v.1. Variants v.1 and v.2 were also characterised by the lowest apparent and particle density. A significantly higher feeding rate resulted in increasing the expansion index, the apparent density, the particle density and water activity of v.3.

Extrusion cooking is a process of continuous cooking, mixing and forming, affecting product chemistry, macroscopic shape and microstructure. Intensive chemical and structural transformations taking place during extrusion make the process an effective way of modifying the physical properties of material, but even small variations in processing conditions may affect process variables as well as product quality considerably (Roudaut et al., 2002; Wolf, 2010). Previous research has shown that extrusion conditions such as feeding rate, barrel temperature, and screw speed affect such properties as density, expansion index, water absorption index (WAI), and water solubility index (WSI) (Ding et al., 2006). The WAI is used to measure the quantity of water absorbed by starch (index of gelatinization), while the WSI, used as an indicator of degree of degradation of molecular components, measures the amount of soluble components released from the starch after extrusion (Ding et al., 2006).

### 3.2. Force-deformation characteristics

Mechanical properties of the extruded bread were investigated using a penetration test and the selected mechanical parameters are presented in Table 2. Figure 1 shows a typical penetration curve of the crisp bread in the force-deformation system and the acoustic signal accompanying this process. The crisp bread variants: 1 and 2 did not differ in terms of the number of force peaks. The lowest number of force peaks was registered for variant 4 bread and the highest one for variant 3 bread. The obtained penetration curves were characterised by an irregular, jagged shape typical for brittle and crisp products (Roudaut et al., 2002). Mean values of the maximal force obtained in the penetration test ranged from 381.6 N for v.2 bread to 849.6 N for v.3 bread (Table 2), which is consistent with results of Marzec et al. (2007) who investigated mechanical properties of extruded wheat and rye bread at different water activities. Literature data indicate that force is often correlated with hardness or tenderness of raw materials (Sealeaw and Schleining, 2011).

Other parameters that have been used to describe crispness of products with a porous structure: are the number of force peaks, the force drop off and linear distance. For v.3 bread (produced with the highest expansion ratio, at the lowest screw speed and the highest feeding rate), the linear distance and the number of force peaks were almost twice as high as for the other bread variants (Table 2). Linear distance as well as the number of force peaks are a measure of the jaggedness of force displacement curves, which can also be described using fractal theory (Roudaut et al.,2002).

### 3.3. Acoustic properties

The impulses of AED acoustic signal coincide with sudden declines of the force (Figure 1). Taniwaki and Kohyama (2012) investigated the texture of potato chips and concluded that the magnitude of the force drop was significantly correlated with associated acoustic events, which can be explained by a mechanism in which the force drop releases the stored strain energy during deformation and some of this energy is released as sound energy. The dry cellular products contain air cavities surrounded by brittle cell walls; applying force to these causes them to bend and break. Each fracture event is accompanied by a drop of the force and an acoustic event (Duizer, 2001; Sealeaw and Schleining, 2011).

At the initial phase of penetration the emission of sound was negligible (Figure 1). In this region, an almost linear increase in force was observed and the structure of the bread was deformed but not damaged. Gondek et al. (2012) used so-called acoustograms to observe this silent stage of penetration in crisp bread v.1, v.2 and v.4. The acoustograms depict the energy and frequency of emitted acoustic emission during the deformation process. Their acquisition requires significant sampling frequency, which is impossible when using the AED.

The number of sound peaks (AED) and the total number of acoustic emission (AE) events are shown in Table 2. The highest number of sound peaks (AED) was detected during deformation of v.3 and v.4 bread. The total number of events (AE) observed for v.3 bread was 516 while, for v.2 it was only 47. Moreover, the acoustic emission peaks of v.3 bread were also characterised by the highest total AE energy (Table 2). The difference between the number of acoustic and mechanical peaks was the result of differences between the sampling rate of the texture analyser (500 Hz) and the acoustic device (44 kHz). The importance of a high sampling rate (greater than 40 kHz) was emphasized by Castro-Prada et al. (2009) and Taniwaki and Kohyama (2012) while investigating mechanical and acoustic properties of biscuits and potato chips. Irrespective of the applied parameters of the extrusion process, the analysed products were characterised by intensive acoustic emission, both in terms of the total AE energy and total number of acoustic events. The registered acoustic emission had a discrete form – a number of short impulses with variable amplitude (Table 2). The average duration of an AE impulse in v.1, v.2 and v.3 breads did not differ and was equal to 85.5 μs. On the contrary, in v.4 bread significantly shorter impulses were registered., i.e. 81.5 μs on average. Both the amplitude and the average energy of a single AE event did not change between bread variants (Table 2).

The AE amplitude-time signals were Fourier transformed to obtain sound spectra. A typical spectrum is shown in Figure 2b, and average spectral characteristic of crisp bread samples are given in Figure 2c. All of the presented spectral characteristics contained the so-called acoustic background, i.e. vibrations generated by the texture analyser registered in spite of using filters. The Fourier transformation confirmed that those vibrations fitted within a frequency range of 0.1-1.0 kHz (an example of background spectrum is presented in Figure 2a). Spectral characteristics of sounds generated during disintegration of food are significant descriptors of food texture, depending on the material morphology. Different food products possess their own individual spectra. In spectral characteristics the predominant sounds with low frequencies of up to 10 kHz are typical of crisp products of cereal origin (Duzier, 2001). The frequency range of the emitted sounds did not differ between bread variants (Figure 2c). Further, for all bread variants the maxima of acoustic energy were noted at frequencies from the same ranges, i.e. 3, 6-7 and 9 kHz. In contrast, significant changes were observed in energy values of the emitted sound. The averaged sound spectrum of v. 3 bread was larger than the three other spectra in the entire range of the analysed frequencies. Similar spectra were obtained by Marzec et al. (2007) when analysing the acoustic emission of crisp bread with different composition. Gondek et al. (2006) obtained the spectral characteristic of corn and wheat breakfast cereals with strong maxima at energy above 14 kHz. Spectra of compressed wheat grain were characterised by the occurrence of two or three maxima at 2-3, 5-7 and 11-13 kHz (Marzec et al., 2011). The sounds generated during biting food products and registered by means of microphones are usually within the range of several to 12-13 kHz, however, a human ear is capable of hearing sounds up to 20 kHz (Duizer, 2001).

### 3.4. Bread microstructure

In the next step, the microstructure of the crisp bread tissue was characterised. More specifically we wanted to investigate whether there are significant microstructural differences between the four bread variants.

Micro-CT cross-section images show the highly porous structure of the crisp breads (Figure 3a). Numerous thin bread walls were present, surrounding a multitude of air inclusions in various shapes, sizes and orientations in 3-D (Figure 3b). Bread v.3 appeared to have thicker walls and larger cells than the other breads. The 3-D datastacks were then quantitatively analysed. Porosity values of the 4 breads were of comparable magnitude, and were over 90% for all the products (Table 1). The closed porosity was considerably lower. Variant 3 had the highest proportion of closed pores, but still only accounting for 0.78% of the volume, indicating that the majority of the pore space was interconnected in 3-D. The cell walls of v.3 (66.2 µm) were significantly thicker than the walls of v.4 (51.2 µm), which itself also had thicker walls than breads v.1 (40.1 µm) and v.2 (38.8 µm) which did not differ significantly. Although porosity values were comparable, it seemed that v.3 consisted of larger air cavities (937 µm diameter on average) than the other breads i.e. variants 1, 2 and 4 (554, 527 and 614 µm diameter respectively). Microstructural differences were also reflected in the bread wall surface area to volume ratio; v.2 had the highest surface area of the bread, compared to its volume (112.4 mm$^{-1}$), indicating a fragile, highly branched structure. Breads v. 1 and v. 2 had wall surface area to volume ratios of 101.8 and 95.3 mm$^{-1}$, respectively. Crisp bread v.3 had a relatively low surface to volume ratio (65.1 mm$^{-1}$). Also in terms of Euler topology, v.3 was characterised by a lower number of interconnections in the wall material compared to the other processing conditions. In terms of (an-)isotropy of the crisp bread material, the different processing conditions showed no major differences, except for bread v. 4 which had a preferred orientation of the walls (Figure 3).

### 3.5. Relationships between structural, mechanical and acoustic parameters

Last, we wanted to investigate whether the differences in mechanical and acoustic parameters of bread were related to their microstructure. We therefore performed a Principal Component Analysis (PCA). This type of study provides a visual representation of the relationships between variables and samples (Figure 4) and provides insights into how measured variables cause some samples to be similar or different from each other.

The first 2 principal componenets (PC's) were able to explain 77% of the variance in all measured variables. This means that relations present in the first 2 PC's could quite well capture the general tendencies present in the data. When taking 7 PC's into account, almost all variance (97%) in the 34 measured variables could be accounted for. The bread samples were more or less grouped according to their preparation procedure in the space of the first 2 PC's. Variant 3 scored high on the 1st PC, while variant 4 in general scored higher on PC 2. Variants 1 and 2 had comparable scores, and were therefore harder to distinguish from each other.

The majority of the variables had a high loading in the first 2 PC's (located between the 2 ellipses in Figure 4). All mechanical variables (maximum force, area under force-deformation curve, linear distance, average drop off and number of force peaks) as well as some acoustic variables (area under acoustic signal curve, number of AED sound peaks, total AE energy, number of AE events and maximum of AED sound peaks) were highly loaded on the first PC. These variables, and thus the first PC, can be related to the crispness of the product. The maximum force was related to the number of acoustic emission events, number of AED sound peaks and total AE energy. Also the Euler number (related to microstructural complexity), bread wall connectivity, thickness of the bread walls and pore sizes were correlated with these "crispness" variables. The area under the acoustic signal curve and mean of sound peaks recorded in the non-contact method by a microphone were related to the number of enclosed pores that were determined by means of X-ray micro-CT. The apparent density of the samples measured by the classic caliper method was highly related to porosity calculated by means of X-ray micro-CT. These variables, however, contributed less to general crispness, and were not correlated with the number of pores or the mean acoustic numbers. Because of the thick walls with the higher number of closed pores, the texture of variant 3 was significantly different from that of the other variants, with higher values of mechanical parameters (maximum force, area below the force deformation curve -penetration work) and also a high number of acoustic emission events as well as sound and force peaks. This indicates the distinctive texture of bread v.3 that was harder and crispier than the other bread samples. Water activity measures were taken into account in the 3rd PC, but seemed to be largely uncorrelated with other variables (data not shown).

Earlier investigations using the AE method demonstrated that among all analysed mechanical and acoustic parameters of crisp bread texture, the number of AE events and the total AE energy were the most strongly correlated with the overall perception of texture quality. These studies addressed the effect of water activity on texture of crisp bread (Gondek and Marzec, 2008). In addition, they showed that the acoustic parameters of texture were stronger correlated with the sensory perception of texture, compared to the mechanical parameters. A very good correlation between total number of sound peaks and sensory crispness was found by Chen et al. (2005) who investigated the texture of biscuits using an acoustic envelope detector (AED).

## 4. Conclusions

The texture parameters of crisp bread as well as porosity and expansion ratio of the finished product were significantly different between bread variants produced with different extrusion process conditions. The breads produced in variable extrusion conditions differed also in terms of water content and water activity as well as WSI and WAI. All analysed samples of bread were products with a crisp texture that emitted audible sounds with a significant intensity that could be registered with a microphone as well as with a contact method. A high number of force and sound peaks and a higher number AE events were due to the porous structure of the material. A higher number of small regular pores facilitates the generation of the sensation of product crispness, whilst large thick-walled pores generate fewer impulses with a higher energy. Out of the proposed production variants the most crispy texture was observed in the bread denoted as v.3 which was confirmed by the results of mechanical acoustic and structural analyses.

***Acknowledgements***

This publication has been produced with the financial support of the European Union (project FP7-226783 - InsideFood). We would like to acknowledge the Hercules Foundation and the Institute for the Promotion of Innovation through Science and Technology (IWT-Vlaanderen, grant number

093469). Thomas Vandendriessche is a post-doctoral fellow of the Research Council of the University of Leuven. The opinions expressed in this document do by no means reflect the official opinion of the European Union or its representatives.

## References

Agbisit, R., Alavi, S., Cheng, E., Herald, T., Trater, A., 2007. Relationships between microstructure and mechanical properties of cellular cornstarch extrudates. Journal of Texture Studies 38, 199–219.

Alamar, M., Vanstreels, E., Oey, M., Molto, E., Nicolaï, B.M., 2008. Micromechanical behaviour of apple tissue in tensile and compression tests: Storage conditions and cultivar effect. Journal of Food Engineering, 86, 324–333.

Babin, P., Della Valle, G., Dendievel, R., Lourdin, D., Salvo, L., 2007. X-ray tomography study of the cellular structure of extruded starches and its relations with expansion phenomenon and foam mechanical properties. Carbohydrate Polymers 68, 329–340.

Castro-Prada, E.M., Primo-Martín, C., Meinders, M.B.J., Hamer, R.J., Van Vliet, T., 2009. Relationship between water activity, deformation speed, and crispness characterization. Journal of Texture Studies 40, 127–156.

Chen, J., Karlsson, C., Povey, M., 2005. Acoustic Envelope Detector for crispness assessment of biscuits. Journal of Texture Studies 36, 139–156.

Ding, Qing-Bo; Ainsworth, P.; Plunkett, A., Tucker, G.; Marson, H., 2006. The effect of extrusion conditions on the functional and physical properties of wheat-based expanded snacks. Journal of Food Engineering 73, 142–148.

Duizer, L.M., 2001. A review of acoustic research for studying the sensory perception of crisp, crunchy and crackly textures. Trends in Food Science and Technology 12, 17–24.

Falcone, P.M., Baiano, A., Zanini, F., Mancini, L., Tromba, G., Montanari, F., Del Nobile, M.A., 2004. A novel approach to the study of bread porous structure: Phase-contrast X-ray microtomography. Journal of Food Science 69, 38–43.

Gondek E., Jakubczyk E., Witrowa-Rajchert D., Antoniuk A., 2012. The influence of different extrusion parameters on acoustic properties of crisp bread. International Conference of Agricultural Engineering, CIGR-AgEng2012, Valencia 8-12 July 2012, Papers Book, ISBN-10 84-615-9928-4, 1–6.

Gondek, E., Lewicki, P.P., Ranachowski, Z., 2006. Influence of water activity on the acoustic properties of breakfast cereals. Journal of Texture Studies 37, 497–515.

Gondek, E., Marzec, A., 2008. Correlations among some selected characteristics of crisp bread texture, determined instrumentally and sensorily. Żywność. Nauka. Technologia. Jakość 4(59), 152–160 (In Polish).

Herremans, E., Jakubczyk, E., Nguyen Do Trong, N., Vanoli, M., Rizzolo, A., Spinelli, L., Torricelli, A., Bongaers, E., Gondek, E., Estrade, P., Saeys, W., Verboven, P., Nicolaï, B.M., 2012. Microstructure-texture relationships of aerated sugar gels: novel measurement techniques for analysis and control. Innovative Food Science and Emerging Technologies, Submitted.

Herremans, E., Verboven, P., Bongaers, E., Estrade, P., Verlinden, B., Wevers, M., Hertog, M.L.A.T.M., Nicolaï, B.M., 2013. Characterisation of 'Braeburn' browning disorder by means of X-ray micro-CT. Postharvest Biology and Technology 75, 114–124.

Lim, K.S., Barigou, M., 2004. X-ray micro-computed tomography of cellular food products. Food Research International 37, 1001–1012.

Luyten, H., Plijter, J.J., van Vliet, T., 2004. Crispy/crunchy crusts of cellular solid foods. A literature review with discussion. Journal of Texture Studies 35, 445–492.

Marzec, A., Lewicki. P. P., Ranachowski, Z., 2007. Influence of water activity on acoustic emission of flat bread extruded bread. Journal of Food Engineering 79, 410422.

Marzec, A., Cacak-Pietrzak, G., Gondek, E., 2011. Mechanical and acoustic properties of spring wheat versus its technological quality factors. Journal of Texture Studies 42, 319–329.

Pareyt, B., Talhaoui, F., Kerckhofs, G., Brijs, K., Goesaert, H., Wevers, M., Delcour, J.A., 2009. The role of sugar and fat in sugar-snap cookies: Structural and textural properties. Journal of Food Engineering 90, 400–408.

Primo-Martín, C., Castro-Prada, E.M., Meinders, M.B.J., Vereijken, P.F.G., van Vliet, T., 2008. Effect of structure in the sensory characterization of the crispness of toasted rusk roll. Food Research International 41, 480–486.

Primo-Martín, C., van Dalen, G., Meinders, M.B.J., Don, A., Hamer, R.H., van Vliet, T., 2010. Bread crispness and morphology can be controlled by proving conditions. Food Research International 43, 207–217.

Roudaut, G., Dacremont, C., Pamies, B. V., Colas, B., Le Meste, M., 2002. Crispness: A critical review on sensory and material science approaches. Trends in Food Science and Technology 13, 217–227.

Saeleaw, M., Schleining, G., 2011. A review. Crispness in dry foods and quality measurements based on acoustic-mechanical destructive techniques. Journal of Food Engineering 105, 387-399.

Szczesniak, A.S., 2002. Texture is a sensory property. Food Quality and Preference 13, 215–225.

Taniwaki, M., Kohyama K., 2012. Mechanical and acoustic evaluation of potato chip crispness using a versatile texture analyzer. Journal of Food Engineering 112, 268–273.

Varela, P., Chen, J., Fiszman, S., Povey, M.J.W., 2006. Crispness assessment of roasted almonds by an integrated approach to texture description: texture, acoustics, sensory and structure. Journal of Chemometrics 20, 311–320.

Verboven, P., Kerckhofs, G., Mebatsion, H.K., Ho, Q., Temst, K., Wevers, M., Cloetens, P., Nicolaï, B.M., 2008. Three-dimensional gas exchange pathways in pome fruit characterized by synchrotron X-ray computed tomography. Plant Physiology 147, 518-527.

Wang, S., Austin, P., Bell, S., 2011. It's a maze: The pore structure of bread crumbs. Journal of Cereal Science 54, 203-210.

Wolf, B., 2010. Polysaccharide functionality through extrusion processing. Current Opinion in Colloid & Interface Science 15, 50-54.

Zdunek, A., Cybulska, J., Konopacka, D., Rutkowski, K., 2011. Evaluation of apple texture with contact acoustic emission detector. A study on performance of calibration models. Journal of Food Engineering 106, 80–87.

Zghal, M.C., Scanlon, M.G., Sapirstein, H.D., 2002. Cellular structure of bread crumb and its influence on mechanical properties. Journal of Cereal Science 36, 167-176.

Table 1. 3-D morphometric parameters for v.1, v.2, v.3 and v.4 crisp bread samples extracted from X-ray micro-CT images. Mean values are presented with their standard error.

| Parameter | Porosity, % | Closed porosity, % | Object surface/volume ratio, $mm^{-1}$ | Bread structure thickness, mm | Pore diameter, mm | Euler number | Structural anisotropy |
|---|---|---|---|---|---|---|---|
| Abbreviation | Porosity | Cl porosity | Bread surf/vol | Wall thickness | Pore size | Euler | Anisotropy |
| Brief definition | Air pore volume (all black pixels after binarisation) divided by total volume of the analysed sample (pores and crisp bread material) | Air volume of closed pores divided by total volume of the analysed sample (pores and crisp bread material). A closed pore in 3-D is a connected assemblage black voxels that is fully surrounded by crisp bread (white) voxels | The surface area of all the bread structures divided by the total volume of the bread within the analysed volume. The 3-D measurements are based on the marching cubes algorithm | Average of the local thickness of the cell space. Calculated by a skeletonisation of the binarised tissue, followed by a sphere fitting algorithm for each voxel of the skeleton | Average of the local thickness of the pores. Calculated by skeletonisation of the binarised tissue, followed by a sphere fitting algorithm for each voxel of the skeleton | Indicator of connectedness of a 3-D complex structure, and a global characterization of topology. Higher values indicate poorly connected structures and lower values for better connected structures | Measure of preferential alignment of structures. This value is scaled from 0 for total isotropy to 1 for total anisotropy. The measurement is based on the mean intercept length and Eigen analysis |
| v.1 | 90.53 ± 0.49 [a] | 0.0921± 0.0074 [b] | 101.8 ± 1.4 [b] | 0.0401 ± 0.0010[c] | 0.554 ± 0.046 [b] | -363x10$^{2}$ ± 55x10$^{2}$ [b] | 0.319 ± 0.015 [b] |
| v.2 | 90.74 ± 0.69 [a] | 0.1019 ± 0.0095 [b] | 112.4 ± 2.4 [a] | 0.0388 ± 0.0016[c] | 0.527 ± 0.026 [b] | -464x10$^{2}$ ± 36x10$^{2}$ [b] | 0.294 ± 0.021 [b] |
| v.3 | 91.71 ± 0.42 [a] | 0.7800 ± 0.3000 [a] | 65.1 ± 1.6 [c] | 0.0662 ±0.0033[a] | 0.937 ± 0.031 [a] | -73x10$^{2}$ ± 11x10$^{2}$ [a] | 0.253 ± 0.046 [b] |
| v.4 | 90.95 ± 0.76 [a] | 0.1120 ± 0.0160 [b] | 95.3 ± 1.4 [b] | 0.0512 ± 0.0025[b] | 0.614 ± 0.055 [b] | -351x10$^{2}$ ± 36x10$^{2}$ [b] | 0.444 ± 0.019 [a] |

Mean values followed by the same small letter (in columns) do not differ significantly at $\alpha = 0.05$

Table 2. Characteristics of functional, mechanical and acoustic properties of crisp bread

| Descriptor | Abbreviation | v.1 | v.2 | v.3 | v.4 |
|---|---|---|---|---|---|
| **Functional properties** | | | | | |
| Water Solubility Index WSI | WAI | 0.26$^{a}$ | 0.36$^{c}$ | 0.31$^{b}$ | 0.34$^{bc}$ |
| Water Adsorption Index WAI | WSI | 4.90$^{b}$ | 4.12$^{a}$ | 3.86$^{a}$ | 4.49$^{ab}$ |
| Water content, % | WC | 6.1$^{b}$ | 5.7$^{a}$ | 7.8$^{c}$ | 5.8$^{ab}$ |
| Water activity | WA | 0.286$^{a}$ | 0.297$^{b}$ | 0.325$^{c}$ | 0.284$^{a}$ |
| Expansion Index | Expansion index | 4.84$^{b}$ | 4.26$^{a}$ | 5.47$^{c}$ | 4.41$^{ab}$ |
| Apparent density, g·cm$^{-3}$ | Apparent density | 0.119$^{a}$ | 0.115$^{a}$ | 0.143$^{c}$ | 0.139$^{b}$ |
| Particle density, g·cm$^{-3}$ | Particle density | 1.032$^{a}$ | 1.028$^{a}$ | 1.181$^{c}$ | 1.073$^{b}$ |
| **Mechanical features of texture** | | | | | |
| Number of force peaks | Peaks M | 20.6$^{b}$ | 19.2$^{b}$ | 45.0$^{c}$ | 9.1$^{a}$ |
| Area under force-deformation curve, N·mm | Area FD | 790.5$^{b}$ | 663.4$^{a}$ | 1447.7$^{d}$ | 908.5$^{c}$ |
| Maximum force, N | Max F | 466.2$^{b}$ | 381.6$^{a}$ | 849.6$^{d}$ | 575.8$^{c}$ |
| Average drop off, N | Drop off | 2.5$^{a}$ | 2.2$^{a}$ | 5.2$^{c}$ | 3.2$^{b}$ |
| Linear distance | Distance FD | 740.9$^{b}$ | 664.7$^{a}$ | 1448.0$^{c}$ | 794.7$^{b}$ |
| **Acoustic Envelope Detector (AED) descriptors** | | | | | |
| Mean of sound peaks AED, dB | Mean peak | 60.9$^{bc}$ | 58.8$^{b}$ | 62.8$^{c}$ | 52.4$^{a}$ |
| Number of sound peaks AED | Peaks AED | 269.5$^{ab}$ | 233.6$^{a}$ | 321.9$^{bc}$ | 295.1$^{b}$ |
| Area under deformation-acoustic signal AED curve, dB·mm | Area AED | 466.5$^{b}$ | 456.4$^{b}$ | 486.2$^{a}$ | 396.3$^{c}$ |
| Maximum of sound peaks AED, dB | Max peak | 92.2$^{ab}$ | 90.4$^{a}$ | 93.0$^{ab}$ | 93.2$^{b}$ |
| **Acoustic Emission (AE) descriptors** | | | | | |
| Total acoustic energy AE, a.u. | Energy AE | 6156.5$^{b}$ | 4713.7 $^{a}$ | 9640.0$^{d}$ | 7568. $^{c}$ |
| AE amplitude, mV | Amplitude | 397.9$^{a}$ | 344.4$^{b}$ | 395.5$^{a}$ | 361.4$^{ab}$ |
| Total number of AE events | Number AE | 97.8$^{b}$ | 47.96$^{a}$ | 516.1$^{d}$ | 365.1$^{c}$ |
| Average duration of AE impulse, µs | Time AE | 86.6$^{a}$ | 83.6$^{ab}$ | 86.2$^{a}$ | 81.5$^{b}$ |
| Average energy of single AE event, mV | Energy single AE | 1240.8$^{a}$ | 1031.2$^{b}$ | 1179.1$^{a}$ | 1008.0$^{b}$ |

Mean values followed by the same small letter (in rows) do not differ significantly at $\alpha = 0.05$

Figure captions:

Figure 1. Relationship between strain vs. force and strain vs. acoustic signal (AED) for crisp bread sample

Figure 2. Spectral characteristic of AE background vibrations (a) and an example (b) as well as average (c) spectra of investigated bread

Figure 3. Reconstructed X-ray micro-CT cross-sections (a) and 3-D structure (b) of crisp bread samples obtained by different processing conditions for v.1, v.2 , v.3 and v.4 samples.

Figure 4 . PCA biplot of the 4 crisp bread variants The first 2 PC’s could explain 77% of the total X-variance. The inner and outer circles on the biplot represent the 70 and 100% explained variance limits. Correlation loadings situated between these circles are considered most important for explaining the variability with respect to the principal components shown.

477 Figure 1

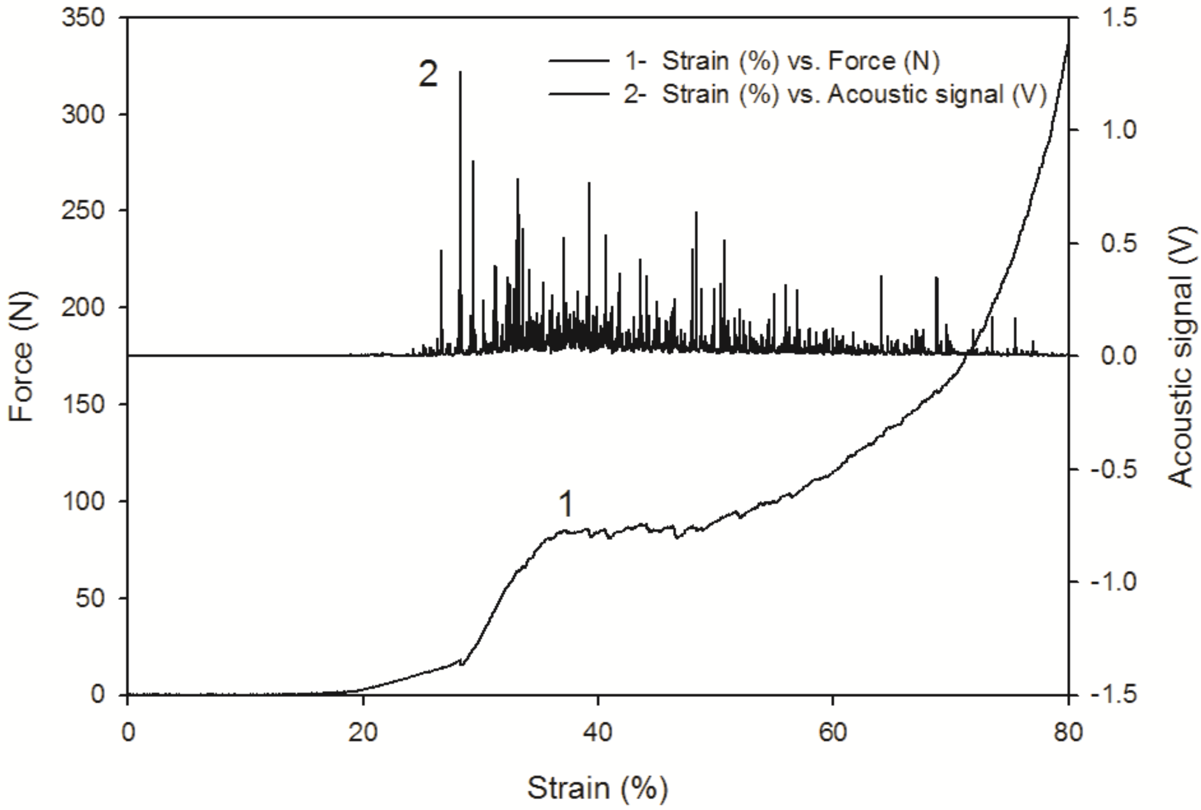

1- Strain (%) vs. Force (N)
2- Strain (%) vs. Acoustic signal (V)
2
1
Force (N)
Acoustic signal (V)
Strain (%)
350
300
250
200
150
100
50
0
1.5
1.0
0.5
0.0
-0.5
-1.0
-1.5
0
20
40
60
80

Figure 2

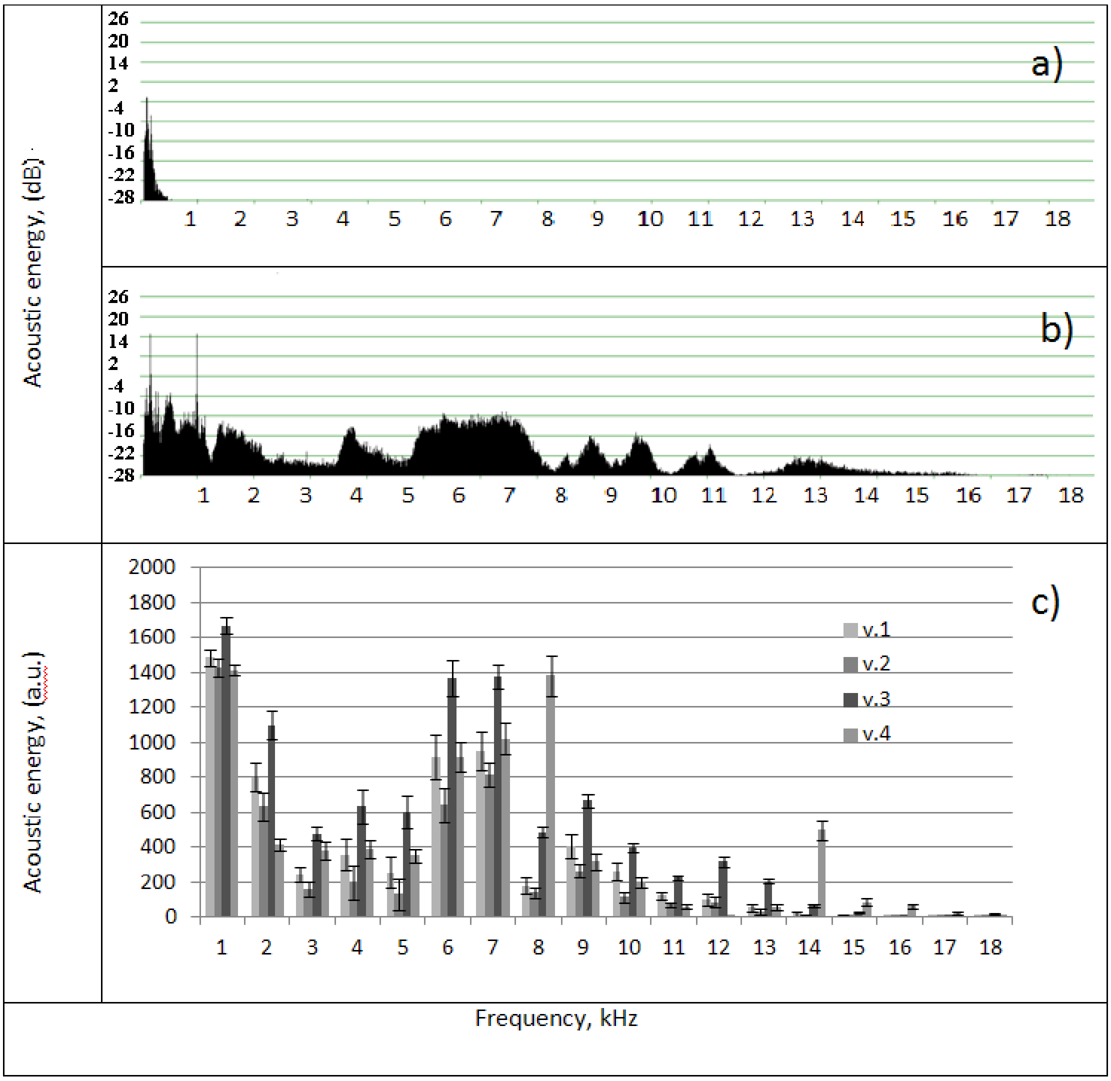

a)
b)
c)
Acoustic energy, (dB)
Acoustic energy, (a.u.)
26
20
14
2
-4
-10
-16
-22
-28
2000
1800
1600
1400
1200
1000
800
600
400
200
0
1 2 3 4 5 6 7 8 9 10 11 12 13 14 15 16 17 18
v.1
v.2
v.3
v.4
Frequency, kHz

Figure 3

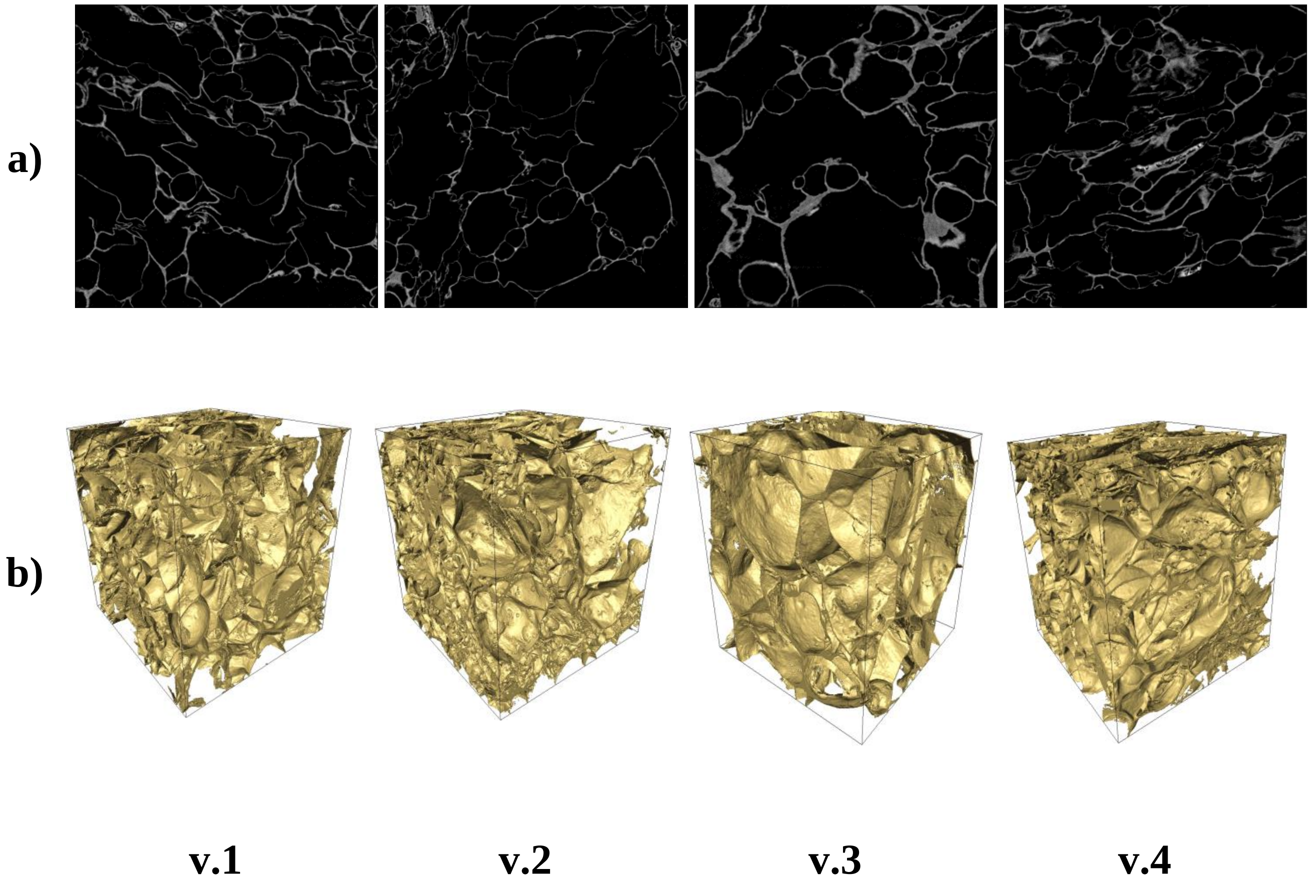

Figure 4

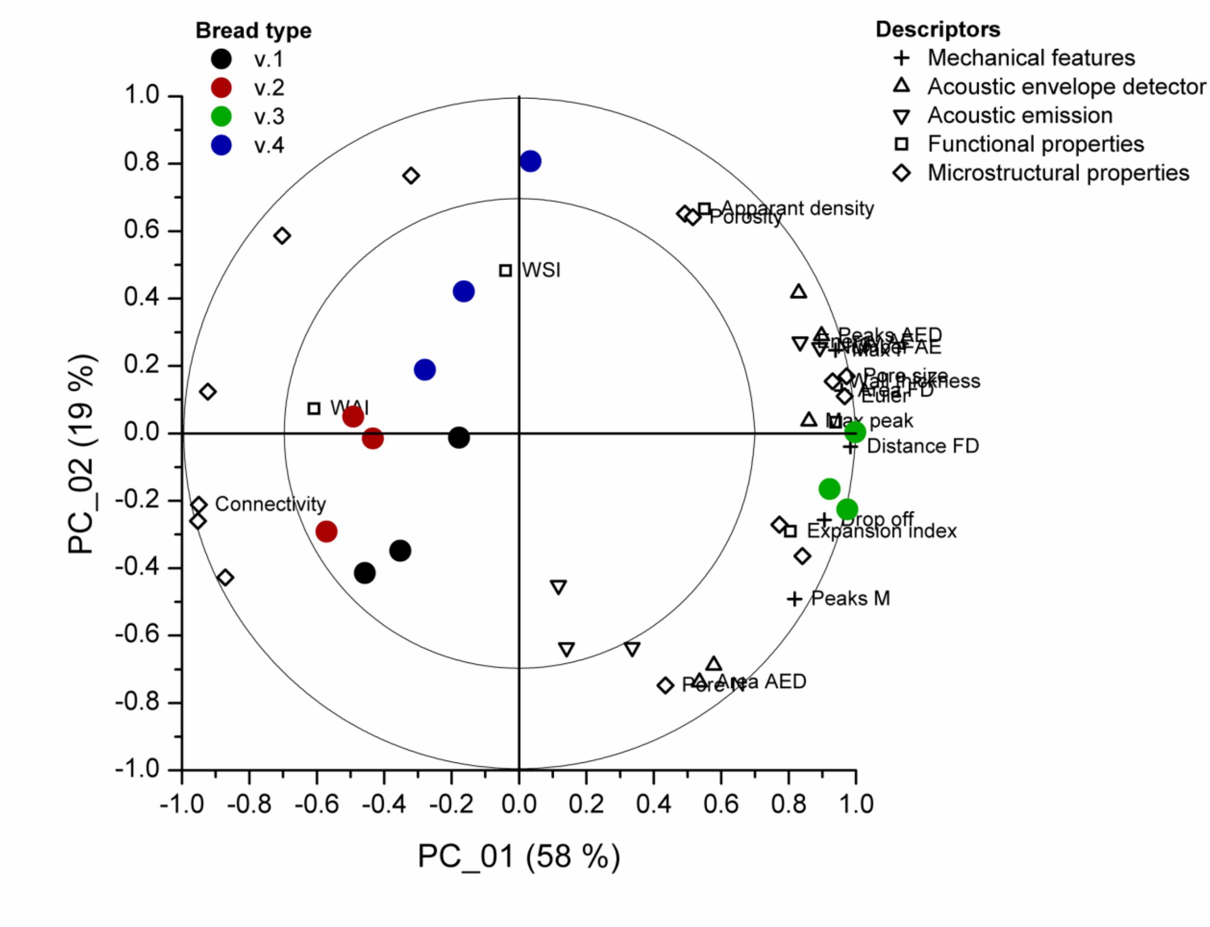

Bread type
v.1
v.2
v.3
v.4
Descriptors
Mechanical features
Acoustic envelope detector
Acoustic emission
Functional properties
Microstructural properties
Apparant density
Porosity
WSI
WAI
Connectivity
Peaks AED
Pore size
Wall thickness
Euler
Max peak
Distance FD
Drop off
Expansion index
Peaks M
Area AED
Pore N
PC_02 (19 %)
PC_01 (58 %)